Proceedings of the 21st ICSMGE, Vienna, Austria, 14 – 19 June 2026. Pistrol, Adam & Schweiger (eds.)
Published by: ÖGG, Austrian Society for Geomechanics, Salzburg, Austria, ISBN 978-3-9503898-4-5
https://doi.org/10.53243/ICSMGE2026-626

Microbial mineralization for enhancing calcium bentonite in sustainable contaminant barriers

Ning-Jun Jiang, Yu Zhang & Xuan-Li Luo
Institute of Geotechnical Engineering, Southeast University, China, Email: Jiangn@seu.edu.cn

ABSTRACT: This study developed a bio-engineered calcium bentonite (BCB) by replacing interlayer Ca^{2+} in calcium bentonite with NH_4^+, a byproduct of microbial mineralization, to enhance its barrier performance of calcium bentonite in soil-bentonite vertical barriers. The hydraulic conductivity of the BCB vertical barriers was reduced from the order of 10^{-9} to 10^{-10} m/s, meeting the impermeability standards required for contaminant barrier applications. Additionally, OH^-, HCO_3^-, and CO_3^{2-}generated in the barriers reacted with Zn^{2+} to form stable precipitates, further inhibiting heavy metal diffusion. This approach was compatible with non-excavation construction methods. The fluidity of BCB slurry prepared by mixing dry components (including enrichment medium, cementitious substrates, and calcium bentonite) with water was prone to flocculation due to chemical stress from added materials. The prepared BCB vertical barrier attained a minimum hydraulic conductivity of 2×10^{-10} m/s without external calcium sources and exhibited good chemical compatibility with $Zn(NO_3)_2$ solutions. Changes in nutrient type had little impact on hydraulic conductivity, whereas the addition of cementitious substrates negatively affected barrier performance by compressing the diffuse double layer through Ca^{2+} and promoting the formation of additional carbonate precipitates, which increased hydraulic conductivity. Moreover, under exposure to high concentrations of $Zn(NO_3)_2$, the BCB barrier's effectiveness diminished when the NH_4^+ produced by the enrichment medium was insufficient. This study provides a sustainable biomodification strategy to promote the application of calcium bentonite in vertical barriers and demonstrates the potential of microbial processes in improving the engineering properties of clay materials.

KEYWORDS: Vertical barrier, microbial mineralization, bentonite, contaminated groundwater, ammonium disposal.

1 INTRODUCTION

The rapid development industrialization and urbanization has exacerbated heavy metal pollution in soils and groundwater in industrialized areas, with contaminant levels often exceeding local background values and posing serious health risks to humans through exposure via soil, water, and the food chain (Su et al. 2022; Xu et al. 2024). Soil-bentonite vertical barriers are widely used to restrict lateral migration of contaminated groundwater, with construction methods categorized into excavation or non-excavation approaches (Bohnhoff & Shackelford 2014; Ma et al. 2024). The excavation method involves stabilizing the trench with bentonite slurry and backfilling it with the soil-bentonite mixture. Non-excavation techniques, such as the trench-and-mix deep-set (TRD) wall method, involve injecting bentonite slurry during in-situ mixing to form a continuous impermeable wall.

Sodium bentonite, known for its strong osmotic swelling, is typically employed in vertical barriers to achieve low hydraulic conductivity (k<1×10^{-9} m/s). In contrast, calcium bentonite, though more abundant and readily available, exhibits limited crystalline swelling and is generally unsuitable for vertical barriers without modification (Yang et al., 2018; Fu et al., 2022). To enhance its barrier performance, calcium bentonite was chemically modified using inorganic or organic additives such as sodium hexametaphosphate (Yang et al., 2018), sodium carboxymethyl cellulose (Fan et al., 2019), and polyanionic cellulose (Shi et al., 2022). These additives improved slurry dispersion, adsorbed heavy metal ions to mitigate the compression of diffuse double layer, and promoted denser microstructures. However, the modification process typically involves multiple steps—heating, stirring, drying, and grinding—which limits scalability for large-scale applications.

Microbially induced carbonate precipitation (MICP) has been shown to effectively reduce the soils' k, as ureolytic bacteria hydrolyze urea into carbonate and ammonium, which react with an external calcium source under alkaline conditions to form $CaCO_3$ precipitates that clog pores and restrict flow (Ma et al. 2021; Xiao et al. 2022; Zhao et al. 2023). This makes MICP a promising method for enhancing the performance of calcium bentonite-based vertical barriers. However, in low-permeability clays like calcium bentonite, grouting and mixing treatments often yield insufficient $CaCO_3$. To address this limitation, this study proposed a bio-engineered calcium bentonite (BCB), utilizing the NH_4^+, a byproduct of MICP, replaced interlayer Ca^{2+} via cation exchange, thereby significantly enhancing the swelling capacity. In addition to reacting with Ca^{2+} to form $CaCO_3$ precipitates, carbonate also reacted with permeating heavy metal ions to inhibit diffusion. In this work, biostimulated MICP was integrated with the TRD method to construct BCB vertical barriers, and the effects of enrichment medium and cementitious substrate concentrations on slurry fluidity and barriers' hydraulic compatibility were evaluated. The findings provided important experimental guidance for optimizing the preparation parameters of BCB vertical barriers.

2 MATERIALS AND METHODS

2.1 *Sand and calcium bentonite*

In this study, model vertical barriers were constructed by river sand and calcium bentonite. The river sand was considered as the in-suit soils with high permeability under aquifer settings (Malusis & McKeehan 2013). The sand, sourced locally form Nanjing, China, was air-dried and passed through a US No. 18 sieve (1 mm). With a fines content (particle size<75 μm) exceeding 30%, it was classified as "sand with fines" based on the Unified Soil Classification System (ASTM, 2017).

The calcium bentonite was supplied by Liaoning Jianping Runying Mining Co., Ltd. Its primary mineralogical composition by dry weight included 71.9% montmorillonite, 13.6% feldspar, 5.0% christobalite, 2.6% quartz, and 2.5% calcite. Due to its high montmorillonite content, the bentonite exhibited a free swell index of 7.8 mL/2g. Prior to use, the bentonite was over-dried and passed through a US No. 200 sieve (0.075 mm).

2.2 *Enrichment medium and cementitious substrates*

Biostimulated MICP technology was employed to promote the proliferation of indigenous ureolytic bacteria within the vertical barriers. The enrichment medium comprised both nutrients and selective substrate (Gomez et al. 2017; Wang et al. 2024; Zhang et al. 2024). In this study, yeast extract and nutrient broth were

used as nutrient sources, and their effects on barrier performance were compared. Yeast extract supplied essential growth components including nitrogen, carbon, amino acids, and cofactors. Nutrient broth offered a broader nutrient profile, consisting of 10 g/L peptone, 3 g/L beef extract, and 5 g/L sodium chloride, with a pH of 7.2. Urea was used as the selective substrate to enrich ureolytic bacteria populations. In addition, the cementation solution contained equimolar concentrations of $CaCl_2$ and urea, a ratio known to provide a suitable balance for efficient microbial mineralization (Tian et al. 2021; Wang et al. 2024). Details on the specific dosage of the enrichment medium and cementitious substrates were provided in section 2.3, which described the preparation of bentonite slurry.

2.3 *Bio-engineered calcium bentonite slurry*

The vertical barriers in this study were prepared using the TRD wall method, a non-excavation construction technique (Ma et al. 2024). This method involves mixing of bentonite slurry with in-situ soils to form a homogeneous barrier wall. The solid components of the BCB slurry included enrichment medium, cementitious substrates, and calcium bentonite. Based on the findings of Yang et al. (2018) on modified calcium bentonite, the calcium bentonite content was set as 20% of the dry weight of river sand. Previous research by the authors (Zhang et al. 2024) demonstrated that an enrichment medium containing 20 g/L nutrient broth and 200 mM urea effectively promoted ureolytic bacteria activity in sand-bentonite mixtures. Building on that benchmark, an additional 200 mM urea was included in the current study to ensure sufficient NH_4^+ production. Accordingly, the nutrient broth and urea contents in the bentonite slurry were 0.8% and 0.9%, respectively, relative to the dry weight of river sand.

Table 1. The solid components of bentonite slurry in vertical barriers.

Specimen nomenclature	Bentonite slurry composition (Percentage of dry sand weight)			
	Nutrient broth/Yeast extract (%)	Urea (%)	$CaCl_2$ (%)	Calcium bentonite (%)
CB	—	—	—	20
CB_NB	0.8	—	—	20
CB_U	—	0.9	—	20
BCB_0Ca	0.8	0.9	—	20
BCB_0Ca(YE)	0.8	0.9	—	20
BCB_0.8Ca	0.8	0.9	0.8	20
BCB_1.6Ca	0.8	1.35	1.6	20
BCB_0Ca(L)	0.4	0.45	—	20
BCB_0Ca(ML)	0.08	0.23	—	20

To avoid the effects of nutrient broth and urea itself on biomodified calcium bentonite, control slurries were prepared with either 0.8% nutrient broth or 0.9% urea alone. Additionally, nutrient broth was substituted with yeast extract to assess whether the NaCl component of nutrient broth influenced biomodification. Cementitious substrates were incorporated into slurry to generate $CaCO_3$ precipitates, aiming to enhance the pore-filling effect in the barrier matrix. Two dosages of $CaCl_2$ were tested—0.8% and 1.6%—corresponding to total urea concentrations of 0.9% and 1.35%, respectively. For comparison, additional barriers without cementitious substrates were formulated with reduced enrichment medium concentrations: 0.4% nutrient broth with 0.45% urea, and 0.08% nutrient broth with 0.23% urea. Table 1 summarizes the solid components of bentonite slurry and the corresponding specimen nomenclatures for the formed vertical barriers. After thoroughly blending the solid components, deionized water was added and stirred at high speed for 10 minutes to create the BCB slurry. A water-to-solid ratio of 1.75 was maintained to ensure sufficient flowability for application via the TRD method (Ma et al. 2024; Jiang et al. 2025).

2.4 *Vertical barrier specimen preparation*

The prepared BCB slurries were thoroughly mixed with river sand and filled into custom molds with a diameter of 50 mm and a height of 25 mm. And the dry density of the vertical barrier specimens was controlled at 1.47 g/cm³ after specimen preparation. The specimens were then biostimulated for 14 days in a standard curing room to form the BCB vertical barriers. Control CB specimens, which did not undergo biostimulation, were also prepared for comparison.

2.5 *Flexible-wall hydraulic conductivity tests*

A series of flexible-wall hydraulic conductivity tests were conducted in accordance with ASTM D5084 (ASTM, 2016) to evaluate the hydraulic performance of various barrier specimens to optimize the dosage of enrichment medium and cementitious substrates in BCB. During the hydraulic conductivity tests, the effective confining stress was maintained at 20 kPa, with a hydraulic gradient of 122 (Bohnhoff & Shackelford 2014; Fu et al. 2022). A two-stage permeation approach was employed to simulate field conditions, wherein the barrier is initially exposed to clean groundwater followed by contaminated groundwater. In this study, tap water was used as a surrogate for clean groundwater, while $Zn(NO_3)_2$ solutions of varying concentrations represented contaminated groundwater (Fu et al. 2022).

When the hydraulic conductivity of barriers permeated with tap water permeation (k_w) was lower than the threshold value for engineering contaminated barriers ($k<1\times10^{-9}$ m/s), the tap water was replaced with $Zn(NO_3)_2$ solutions to continue testing. During the $Zn(NO_3)_2$ permeation phase, effluent samples were collected and analyzed for pH, electrical conductivity, and Zn concentration. Once these chemical parameters stabilized within a range of 0.9–1.1, relative to the corresponding values in the permeating solution, the barriers were considered to have reached chemical equilibrium. At this stage', the hydraulic conductivity under $Zn(NO_3)_2$ exposure (k_c) was determined (ASTM, 2011).

2.6 *X-ray fluorescence and carbonate content analysis*

X-ray fluorescence analysis was employed to quantify the metal oxide composition of vertical barriers before and after biomodification. Oven-dried BCB and CB samples were ground into fine powder and analyzed using a wavelength dispersive X-ray fluorescence spectrometer. The carbonate contents of all barriers were determined using a modified acid dissolution method (Ma et al. 2021). During the washing process, low-speed quantitative filter papers were used to retain fine particles. The carbonate content was then calculated based on the dry weight loss of the samples following acid treatment.

3 RESULTS AND ANALYSIS

Figure 1 presents the flow spread diameter results for various bentonite slurries. The diameter of all bentonite slurries ranged from 185 to 215 mm, falling within the recommended flowability range for bentonite slurries (150~250 mm) (Jiang et al. 2025). The slurry prepared using only deionized water (CB) exhibited a diameter of 215 mm. The addition of either nutrient broth or urea reduced the diameter to approximately 200 mm, likely due to enhanced flocculation of bentonite particles

induced by the chemical constituents of these additives. When the full enrichment medium (nutrient broth or yeast extract combined with urea) was introduced, the diameter further decreased. However, the type of nutrient had minimal influence on slurry fluidity, as evidenced by comparable diameters of 192 mm and 191 mm for nutrient broth and yeast extract, respectively. In contrast, the addition of cementitious substrates significantly reduced the diameter. The presence of free Ca^{2+} notably decreased the dispersibility of the bentonite slurry by compressing the diffuse double layer surrounding bentonite particles (Ren et al. 2024). The diameters of slurries containing 0.8% and 1.6% $CaCl_2$ dropped to 189 mm and 185mm, respectively. Conversely, lowering the enrichment medium concentration improved the fluidity of bentonite slurry.

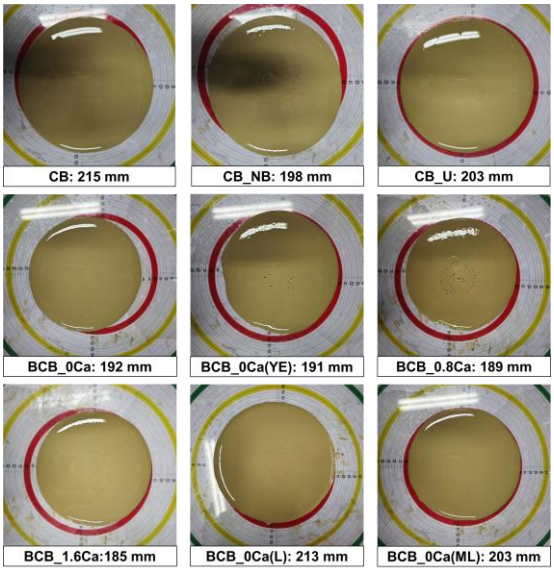

Figure 1. Flow spread diameter of various bentonite slurries

The vertical barrier specimens, formed by mixing these slurries with river sand, were subjected to flexible-wall hydraulic conductivity tests following a 14-day standard curing period. As shown in Figure 2, the k_w of the CB was measured at 2.52×10^{-9} m/s, exceeding the k limit for engineering contaminant barriers ($k<1\times10^{-9}$ m/s). Specimens with added nutrient broth or urea—CB_NB and CB_U—exhibited even higher k_w values of 3.51×10^{-9} m/s and 5.85×10^{-9} m/s, respectively. This increase was expected, as the chemical stress introduced by these additives likely inhibited the swelling behavior of highly active bentonite (Shackelford & Sample-Lord 2014). In contrast, the biostimulated BCB specimens, BCB_0Ca and BCB_0Ca(YE), showed a significant reduction in k_w, achieving k_w values as low as 2×10^{-10} m/s. This improvement was attributed to NH_4^+ generated from MICP undergoing cation exchange with Ca^{2+} in the bentonite interlayers. When bentonite interlayers are dominated by monovalent cations, such as Na^+ or NH_4^+, the hydrated bentonite exhibits enhanced osmotic swelling compared to the limited crystalline swelling of calcium bentonite (Setz et al. 2017). This increased swelling capacity significantly reduced the k_w of BCB. X-ray fluorescence analysis further confirmed the occurrence of ammonium modification. As shown in Table 2, the CaO, Na_2O, and MgO contents in BCB_0Ca decreased by 0.48%, 0.35%, and 0.46%, respectively, compared to the unmodified CB (Gautier et al. 2010).

Figure 3(a) illustrates the effect of varying cementitious substrates concentrations on the k of BCB specimens. After stabilizing under tap water permeation, the specimens were sequentially exposed to $Zn(NO_3)_2$ solutions at concentrations of

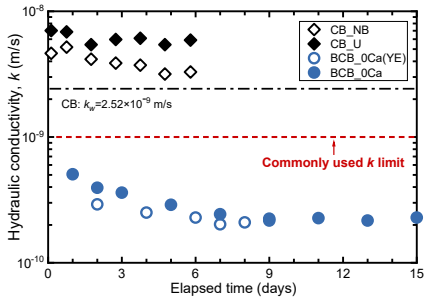

Figure 2. Hydraulic conductivity of CB and BCB specimens under tap water permeation conditions.

Table 2. Chemical composition of powder CB and BCB specimens

Metal oxide (%)	CB	BCB_0Ca
SiO_2	67.54	69.91
Al_2O_3	17.63	16.28
K_2O	3.19	3.41
CaO	2.71	2.23
Na_2O	2.21	1.86
MgO	1.39	0.93
Fe_2O_3	3.90	3.91
Others	1.43	1.48

20 mM, 100 mM, and 300 mM. Figures 3(b)-(d) present the evolution of pH, electrical conductivity, and Zn concentration during the flexible-wall hydraulic conductivity tests. The BCB specimen without cementitious substrates, designated as BCB_0Ca(YE), exhibited a k_w of 2.14×10^{-10} m/s. On the contrary, the k_w values of BCB specimens with added 0.8% and 1.6% $CaCl_2$—BCB_0.8Ca and BCB_1.6Ca—were higher than that of BCB_0Ca(YE), reaching 2.24×10^{-10} m/s and 2.89×10^{-10} m/s, respectively. The elevated k_w values also corresponded to their low fluidity of slurries, as shown in Figure 4. Upon exposure to 20 mM $Zn(NO_3)_2$, BCB_0Ca(YE) exhibited a notable reduction in k_c, with its average value declining to 1.37×10^{-10} m/s within the first 5 days of permeation. Concurrently, electrical conductivity dropped from 2.34 ms/cm to 1.77 ms/cm, while Zn concentration in the effluent stabilized around 6.5 mM. For BCB_0.8Ca and BCB_1.6Ca, their k_c initially decreased during early $Zn(NO_3)_2$ permeation, the Zn concentrations of these two specimens increased to 8.33 mM and 9.52 mM, respectively, by the third day. These results suggested that although the addition of cementitious substrates could generate carbonate content, which contributed to pore filling within the barrier, excessive carbonate content also diminished the swelling potential of bentonite (Zhao et al. 2021), resulting in an increased k_w. This characteristic is often leveraged to control deformation in expansive soil embankments and slopes (Tiwari et al. 2021). On the other hand, given the limited production of carbonate via urea hydrolysis, the absence of additional calcium sources in the BCB_0Ca(YE) specimens allowed the available carbonate to not only bound with exchanged Ca^{2+} but also reacted with Zn^{2+} in the permeating solution. During the first 5 days of $Zn(NO_3)_2$ permeation, the pH in BCB_0Ca(YE) remained between 8.50 and 8.62, creating an alkaline environment favorable for the formation of Zn precipitates such as $Zn(OH)_2$, $Zn_2(OH)_2CO_3$, and $ZnCO_3$ (Jiang et al. 2019). These reactions significantly inhibited the diffusion of Zn^{2+}. In contrast, the higher k_c observed in BCB_0.8Ca and BCB_1.6Ca specimens accelerated the Zn^{2+} migration, and the remaining carbonate ions—after reacting with Ca^{2+}—were insufficient to effectively suppress Zn^{2+} diffusion.

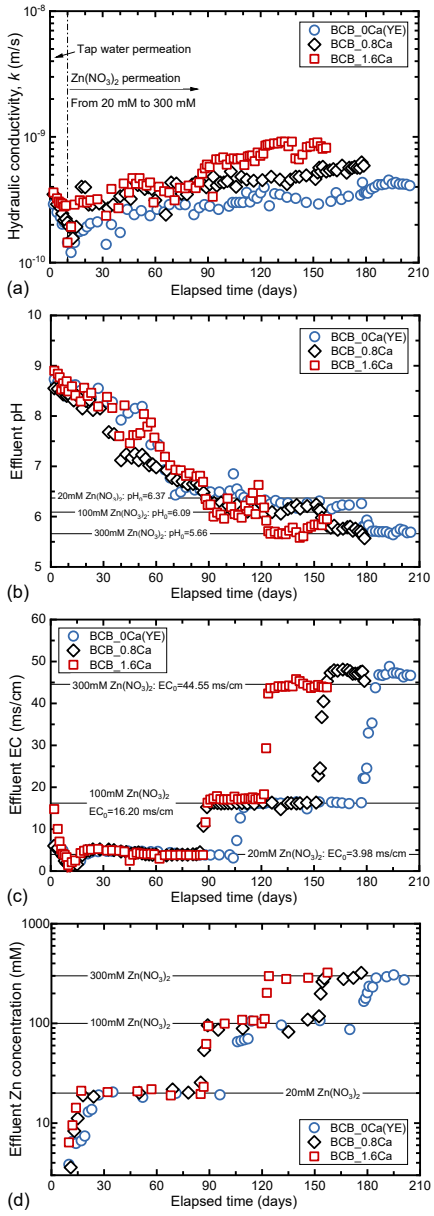

Figure 3. Effect of cementitious substrates concentration on the chemical compatibility of BCB specimens: (a) hydraulic conductivity; (b) pH; (c) electrical conductivity; and (d) Zn concentration.

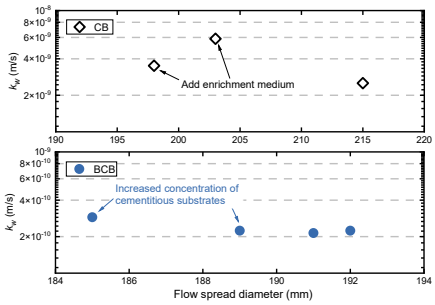

Figure 4. Relationship between flow spread diameter and k_w.

As the $Zn(NO_3)_2$ permeation continued, the accumulation of H^+ in the solution caused a gradual decline in pH, which inhibited the formation of Zn precipitates through microbial mineralization. Consequently, Zn^{2+} transport through the barrier was primarily governed by chemical diffusion. During this process, Zn^{2+} replaced exchangeable NH_4^+ and Na^+ within the BCB, reducing the diffuse double layer thickness of bentonite, which in turn enlarged pore sizes and led to an increase in k_c (Fu et al. 2022). Once pH, electrical conductivity, and Zn concentration in the effluent reached chemical equilibrium, the k_c values for BCB_0Ca(YE), BCB_0.8Ca, and BCB_1.6Ca permeated with 20 mM $Zn(NO_3)_2$ increased to 2.79×10^{-10}m/s, 3.88×10^{-10}m/s, and 4.06×10^{-10} m/s, respectively. Further increases in $Zn(NO_3)_2$ concentration resulted in additional increases in k_c, though all values remained below the permissible limit of 1×10^{-9} m/s.

Table 3. Results of flexible-wall hydraulic conductivity tests.

Vertical barrier specimen	Permeant Liquid	Elapsed Time (days)	k value ($\times10^{-10}$ m/s)	k_c/k_w
CB	Tap water	—	25.20	—
CB_NB	Tap water	5.8	35.10	—
CB_U	Tap water	5.8	58.50	—
BCB_0Ca	Tap water	15	2.24	—
BCB_0Ca(YE)	Tap water	9	2.14	—
	20 mM $Zn(NO_3)_2$	93	2.79	1.30
	100 mM $Zn(NO_3)_2$	75	3.40	1.59
	300 mM $Zn(NO_3)_2$	28	4.18	1.95
BCB_0.8Ca	Tap water	10	2.24	—
	20 mM $Zn(NO_3)_2$	72	3.88	1.73
	100 mM $Zn(NO_3)_2$	66.2	4.80	2.14
	300 mM $Zn(NO_3)_2$	26.3	5.88	2.63
BCB_1.6Ca	Tap water	9	2.89	—
	20 mM $Zn(NO_3)_2$	75	4.06	1.40
	100 mM $Zn(NO_3)_2$	33.1	7.02	2.43
	300 mM $Zn(NO_3)_2$	37.5	8.43	2.92
BCB_0Ca(L)	Tap water	9.9	2.05	—
	100 mM $Zn(NO_3)_2$	25.6	5.41	2.64
BCB_0Ca(ML)	Tap water	9.1	5.98	—
	100 mM $Zn(NO_3)_2$	22.4	10.8	1.81

As summarized in Table 3, the results from flexible-wall hydraulic conductivity tests indicate that the incorporation of cementitious substrates adversely affected the chemical compatibility of the barriers. This is evidenced by an increasing compatibility ratio (k_c/k_w) with rising cementitious substrates concentration; for example, under 300 mM $Zn(NO_3)_2$ permeation, k_c for BCB_0Ca(YE) increased by 1.95 times relative to k_w, while BCB_1.6Ca showed an increase of 2.92 times. The pronounced influence of cementitious substrates concentration on chemical compatibility highlights the importance of optimizing formulation parameters for barrier preparation. In addition, from an engineering perspective, when the calcium content in mixing water is elevated, the addition of urea could help mitigate adverse effects on hydraulic performance. However, if calcium content exceeds 1.6%, the use of such water is not recommended for the construction of BCB vertical barriers.

Figure 5 shows the effect of further reducing the enrichment medium concentration on the k of BCB_0Ca specimens. The results indicated that the k_w of BCB_0Ca(L)

containing 0.4% nutrient broth and 0.45% urea was 2.05×10^{-10} m/s, which close to the k_w of BCB_0Ca and BCB_0Ca(YE) specimens with higher enrichment medium concentrations. However, upon exposure to a 100 mM $Zn(NO_3)_2$ solution, the k_c of BCB_0Ca(L) increased by 2.64 times, reaching 5.41×10^{-10} m/s. In contrast, the k_c values for BCB_0Ca and BCB_0Ca(YE) under the same $Zn(NO_3)_2$ permeation were lower, at 3.40×10^{-10} m/s and 4.80×10^{-10} m/s, respectively. This difference may be attributed to the higher concentrations of NH_4^+ generated in BCB_0Ca and BCB_0Ca(YE), which likely enhanced the ammonium modification of calcium bentonite. Conversely, the BCB_0Ca(ML) specimen, prepared with only 0.08% nutrient broth and 0.23% urea, exhibited poor ammonium modification. Its k_w was 5.98×10^{-10} m/s, and its k_c increased to 1.08×10^{-9} m/s under 100 mM $Zn(NO_3)_2$ permeation—exceeding the k limit for containment barrier applications.

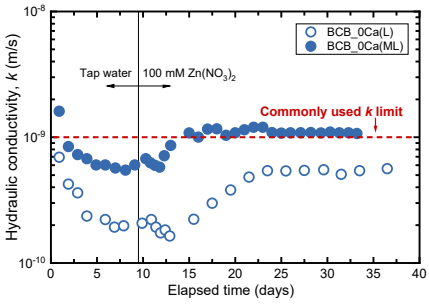

Figure 5. Effect of enrichment medium type on the hydraulic conductivity of BCB specimens.

4 DISCUSSION

The core mechanism of the BCB vertical barriers involved the replacement of interlayer Ca^{2+} in calcium bentonite by NH_4^+, thereby significantly enhancing the swelling capacity. Simultaneously, carbonate reacted with permeating Zn^{2+} under alkaline conditions to form Zn precipitates, further hindering its diffusion. Owing to these synergistic effects, the k_w values of BCB_0Ca, BCB_0Ca(YE), BCB_0Ca(L), and BCB_0Ca(ML) were reduced to the order of 10^{-10} m/s. And these specimens also showed slight reductions in k_c during the initial permeation of $Zn(NO_3)_2$ solution and maintained good chemical compatibility even under exposure to $Zn(NO_3)_2$ concentrations as high as 300 mM.

During the ammonium modification, displaced Ca^{2+}, Mg^{2+}, and CO_3^{2-} underwent mineralization reactions, resulting in increased carbonate contents in all four BCB specimens (Figure 6). The carbonate contents had the trend that positively correlated with the concentration of enrichment medium: BCB_0Ca and BCB_0Ca(YE) showed an approximate increase of 0.3%, while BCB_0Ca(L) and BCB_0Ca(ML) exhibited only about 0.14%. This difference is attributed to the higher

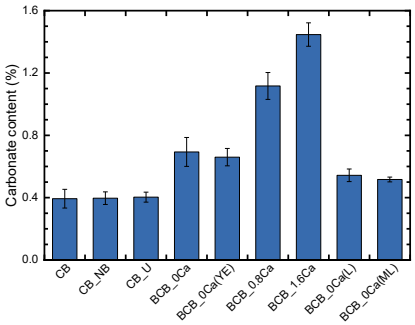

Figure 6. Average carbonate content of CB and BCB vertical barriers under different conditions.

NH_4^+ production under elevated enrichment conditions, which displaced more Ca^{2+} and Mg^{2+} for subsequent mineralization. Additionally, the thorough ammonium modification also resulted in lower hydraulic performance. Notably, while the addition of calcium sources was expected to increase $CaCO_3$ precipitation and further reduce k, the opposite effect was observed. Additional calcium exacerbated diffuse double layer compression, enlarged pore spaces (Zhang et al., 2024), and excessive $CaCO_3$ precipitation hindered the swelling of hydrated bentonite (Zhao et al. 2021). Consequently, BCB_0.8Ca and BCB_1.6Ca exhibited higher k values compared to BCB_0Ca, which had no added calcium source.

These findings highlight the importance of selecting appropriate enrichment medium concentrations and carefully managing calcium input during BCB barrier construction. The design must consider the contamination level of the groundwater and the calcium content of the mixing water (Norris et al. 2018). Figure 7 gives the mechanisms through which contaminant–calcium bentonite–MICP interactions influence BCB's barrier performance. Future research should aim to further optimize the preparation parameters of BCB vertical barriers. Particular attention should be paid to evaluating the effects of varying types and concentrations of contaminated groundwater, as well as the in-soil contamination level, on the engineering behavior and long-term performance of BCB barriers.

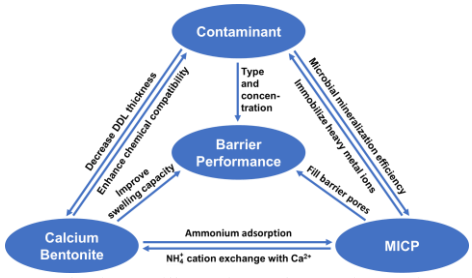

Figure 7. Mechanism illustrating how interactions among contaminant, calcium bentonite, and MICP influence BCB's barrier performance.

5 CONCLUSIONS

This study addressed the complex inorganic and organic modification processes required for calcium bentonite -based vertical barriers by proposing a novel biomodified approach that utilized NH_4^+, a byproduct of microbial mineralization, to replace Ca^{2+} in the calcium bentonite interlayer via cation exchange. The resulting NH_4^+-dominated interlayer significantly enhanced the swelling behavior of hydrated bentonite, allowing the k of BCB vertical barriers to meet the engineering standards for contaminant barriers, with k values reaching the 10^{-10} m/s range. In addition to improving swelling, the OH^-, HCO_3^-, and CO_3^{2-} produced in the BCB reacted with permeating Zn^{2+} under alkaline conditions to form stable precipitates such as $Zn(OH)_2$, $Zn_2(OH)_2CO_3$, and $ZnCO_3$, thereby inhibiting the diffusion of Zn^{2+}.

This biomodification approach proved particularly suitable for non-excavation construction methods, such as TRD method. The enrichment medium, cementitious substrates, and bentonite were mixed in a dry state and subsequently combined with water to produce a BCB slurry. At a liquid-to solid of 1.75 the flow spread diameter of the slurries ranged from 185 to 215 mm, satisfying the fluidity requirements for TRD method (150~250 mm). However, the concentrations of enrichment medium and cementitious substrates significantly influenced both the fluidity by promoting bentonite flocculation or compressing the diffuse double layer. In terms of k, the use of nutrient broth (0.8%

dry weight of in-situ soil) and urea (0.9%) as the enrichment medium reduced the k of the CB barriers by nearly an order of magnitude. Replacing nutrient broth with yeast extract resulted in negligible changes in k. Conversely, the addition of extra cementitious substrates increased the k of the BCB and shortened the breakthrough time of Zn^{2+}. When the enrichment medium concentration was reduced, the k_w of the BCB remained below 1×10^{-9} m/s; however, the barrier function failed under permeation by highly concentrated $Zn(NO_3)_2$ solutions. This occurred because, under standard preparation conditions, effective ammonium modification required a high concentration of enrichment medium to supply sufficient NH_4^+.

This study provided important guidance for the practical construction of BCB vertical barriers by systematically optimizing key preparation parameters. The approach of biomodification in clay minerals to improve engineering properties offered new insights for geotechnical engineers in addressing clay-related issues.

6 ACKNOWLEDGEMENTS

This work was financially supported by the Key R&D Program Social Development Project of Jiangsu Province (Grant No. BE2023800), Natural Science Foundation of China (Grant No. 42377166), and Postgraduate Research & Practice Innovation Program of Jiangsu Province (Grant No. KYCX24_0441).

7 REFERENCES

ASTM (American Society for Testing and Materials). 2011. Standard test method for hydraulic conductivity compatibility testing of soils with aqueous solutions. ASTM D7100. West Conshohocken, PA: ASTM.

ASTM (American Society for Testing and Materials). 2016. Standard test methods for measurement of hydraulic conductivity of saturated porous materials using a flexible wall permeameter. ASTM D5084. West Conshohocken, PA: ASTM.

ASTM (American Society for Testing and Materials). 2017. Standard practice for classification of soils for engineering purposes (Unified Soil Classification System). ASTM D2487-17. West Conshohocken, PA: ASTM.

Bohnhoff, G.L., and Shackelford, C.D. 2014. Hydraulic conductivity of polymerized bentonite-amended backfills. *Journal of Geotechnical and Geoenvironmental Engineering*. 140(3), 04013028.

Fan, R.D., Liu, S.Y., Du, Y.J., Reddy, K.R., and Yang, Y.L. 2019. Chemical compatibility of CMC-treated bentonite under heavy metal contaminants and landfill leachate. *Proceedings of the 8th International Congress on Environmental Geotechnics, Volume 2: Towards a Sustainable Geoenvironment*. Springer, 2018.

Fu, X.L., Shen, S.Q., Reddy, K.R., Yang, Y.L., and Du, Y.J. 2022. Hydraulic conductivity of sand/biopolymer-amended bentonite backfills in vertical cutoff walls permeated with lead solutions. *Journal of Geotechnical and Geoenvironmental Engineering*. 148(2), 04021186.

Gautier, M., Muller, F., Le Forestier, L., Beny, J.M., and Guégan, R. 2010. NH_4-smectite: Characterization, hydration properties and hydro-mechanical behaviour. *Applied Clay Science*. 49(3), 247–254.

Gomez, M.G., Anderson, C.M., Graddy, C.M., DeJong, J.T., Nelson, D.C., and Ginn, T.R. 2017. Large-scale comparison of bioaugmentation and biostimulation approaches for biocementation of sands. *Journal of Geotechnical and Geoenvironmental Engineering*. 143(5), 04016124.

Jiang, N.J., Liu, R., Du, Y.J., and Bi, Y.Z. 2019. Microbial induced carbonate precipitation for immobilizing Pb contaminants: Toxic effects on bacterial activity and immobilization efficiency. *Science of the Total Environment.* 672, 722–731.

Jiang, Z.Y., Fu, X.L., Jin, F., Che, C., Li, Z.Y., Cai, G., and Du, Y.J. 2025. SEBS-amended in-situ mixed wall material for diesel-contaminated groundwater management. *Journal of Hazardous Materials*. 491, 137966.

Malusis, M.A., and McKeehan, M.D. 2013. Chemical compatibility of model soil-bentonite backfill containing multiswellable bentonite. *Journal of Geotechnical and Geoenvironmental Engineering*. 139(2), 189–198.

Ma, G., He, X., Jiang, X., Liu, H., Chu, J., and Xiao, Y. 2021. Strength and permeability of bentonite-assisted biocemented coarse sand. *Canadian Geotechnical Journal*. 58(7), 969–981.

Ma, T.X., Zhuang, H., Wang, S., Ni, H., Pan, Y., Feng, Y.S., Liu, D.F., and Du, Y.J. 2024. Field trial of constructing vertical barriers using small-scale TRD method at an organic compounds-contaminated site. *Chinese Journal of Geotechnical Engineering*. DOI: 10.11779/CJGE20240302 (in Chinese).

Norris, A., Di Emidio, G., Malusis, M.A., and Replogle, M. 2018. Modified bentonites for soil-bentonite cutoff wall applications with hard mix water. *Applied Clay Science*. 158, 226–235.

Ren, G., Meng, M., Fan, H., Wen, J., Zhang, J., Zhao, G., and He, X. 2024. Calcium ions and calcium carbonate: key regulators of the enzymatic mineralization for soil dispersivity control. *Acta Geotechnica*. 19(10), 6661–6682.

Setz, M.C., Tian, K., Benson, C.H., and Bradshaw, S.L. 2017. Effect of ammonium on the hydraulic conductivity of geosynthetic clay liners. *Geotextiles and Geomembranes*. 45(6), 665–673.

Shackelford, C.D., and Sample-Lord, K.M. 2014. Hydraulic conductivity and compatibility of bentonite for hydraulic containment barriers. In: *From soil behavior fundamentals to innovations in geotechnical engineering: Honoring Roy* E. Olson, 370–387.

Shi, F.J., Feng, S.J., Zheng, Q.T., Zhang, X.L., and Chen, H.X. 2022. Effect of polyanionic cellulose modification on properties and microstructure of calcium bentonite. *Applied Clay Science*. 228, 106633.

Tian, Z., Tang, X., Li, J., Xiu, Z., and Xue, Z. 2021. Influence of the grouting parameters on microbially induced carbonate precipitation for soil stabilization. *Geomicrobiology Journal*. 38(9), 755–767.

Tiwari, N., Satyam, N., and Sharma, M. 2021. Micro-mechanical performance evaluation of expansive soil biotreated with indigenous bacteria using MICP method. *Scientific Reports*. 11(1), 10324.

Wang, Y.J., Chen, W.B., Yin, J.H., Han, X.L., Zhang, Y., Du, Y.J., and Jiang, N.J. 2024. Role of biochar in drained shear strength enhancement and ammonium removal of biostimulated MICP-treated calcareous sand. *Journal of Geotechnical and Geoenvironmental Engineering*. 150(2), 04023140.

Xiao, Y., He, X., Zaman, M., Ma, G.L., and Zhao, C. 2022. Review of strength improvements of biocemented soils. *International Journal of Geomechanics*. 22(11), 03122001.

Xu, D., Wang, Z., Tan, X., Xu, H., Zhu, D., Shen, R., and Yang, Z. 2024. Integrated assessment of the pollution and risk of heavy metals in soils near chemical industry parks along the middle Yangtze River. *Science of the Total Environment*. 917, 170431.

Su, C., Meng, J., Zhou, Y., Bi, R., Chen, Z., Diao, J., and Wang, T. 2022. Heavy metals in soils from intense industrial areas in south China: Spatial distribution, source apportionment, and risk assessment. *Frontiers in Environmental Science*. 10, 820536.

Yang, Y.L., Reddy, K.R., Du, Y.J., and Fan, R.D. 2018. Short-term hydraulic conductivity and consolidation properties of soil-bentonite backfills exposed to CCR-impacted groundwater. *Journal of Geotechnical and Geoenvironmental Engineering*. 144(6), 04018025.

Zhao, C., Xiao, Y., He, X., Liu, H., Liu, Y., & Chu, J. (2023). Influence of injection methods on bio-mediated precipitation of carbonates in fracture-mimicking microfluidic chip. *Géotechnique*, 75(2), 153-165.

Zhao, Y., Zhang, P., Fang, H., Guo, C., Zhang, B., and Wang, F. 2021. Bentonite-assisted microbial-induced carbonate precipitation for coarse soil improvement. *Bulletin of Engineering Geology and the Environment*. 80(7), 5623–5632.

Zhang, Y., Xu, X.R., Liu, S.Q., Wang, Y.J., Du, J., and Jiang, N.J. 2024. Bacterial activity and cementation pattern in biostimulated MICP-treated sand-bentonite mixtures. *Journal of Rock Mechanics and Geotechnical Engineering*. 16(12), 5121–5134.